

Helical Bis[2-(ferrocenylmethylenamino)benzenethiolato] Metal(II) Complexes ($M = Ni, Zn$ or Pd) and a Related Mercury(II) Complex[†]

Tatsuya Kawamoto and Yoshihiko Kushi *†

Coordination Chemistry Laboratories, Institute for Molecular Science, Myodaiji, Okazaki 444, Japan

The reaction between M^{2+} ($M = Ni, Zn$ or Pd) and 2-(ferrocenyl)benzothiazoline in ethanol affords the trinuclear complexes $[M(fabt)_2]$ [$fabt = 2\text{-}(ferrocenylmethylenamino)benzenethiolato$]. Interaction of $[Ni(fabt)_2]$ or $[Zn(fabt)_2]$ with $HgCl_2$ gives the complex *trans*- $[Hg(fabt)_2]$. Infrared, 1H NMR, electronic absorption and cyclic voltammetric data are given. The crystal structures of $[Ni(fabt)_2]$ and $[Pd(fabt)_2]$ show a helical geometry, which is also confirmed for distorted-tetrahedral $[Zn(fabt)_2]$.

Helicity is a widespread phenomenon in natural systems and molecular helicity is well known in double-helical compounds,¹ but rare in monohelical metal complexes.^{2,3} In order to delineate the features of the driving force leading to molecular helicity, we have investigated a series of N_2S_2 donor atom sets with two ferrocene units.

In this paper we describe the synthesis, crystal structures, 1H NMR data, and cyclic voltammograms of the complexes $[M(fabt)_2]$ [$M = Ni^{II}, Zn^{II}$ or Pd^{II} ; $fabt = 2\text{-}(ferrocenylmethylenamino)benzenethiolato$] showing monohelical chirality. In addition we have carried out the reaction of these complexes with $HgCl_2$ to examine the co-ordination ability of the sulfur atoms present. The reaction product with Ni^{II} and Zn^{II} was a trinuclear mercury(II) complex, in which the mercury atom is in a linear *trans*- $[Hg^{II}S_2]$ type co-ordination. The structure of $[Pd(fabt)_2]$ was recently communicated.³

Experimental

Reactions were normally carried out under argon; solvents were thoroughly degassed by argon purge. Methanol and ethanol were dried over molecular sieve type 3A. Chloroform was dried over $CaCl_2$. Unless otherwise stated, commercial grade chemicals were used without further purification.

Methods.—Infrared spectra were obtained on a Shimadzu FTIR-8100 instrument ($4000\text{--}400\text{ cm}^{-1}$) as KBr discs, NMR spectra on a JEOL GX 400 instrument using tetramethylsilane as internal standard ($\delta 0$), and UV/VIS spectra on a Hitachi U-3400 spectrophotometer. Cyclic voltammetry was performed in a three-electrode cell with a glassy-carbon disc as working electrode, a platinum wire as counter electrode and a $Ag-AgCl$ reference electrode, in acetonitrile containing 0.1 mol dm^{-3} tetra-*n*-butylammonium tetrafluoroborate. Acetonitrile was distilled from CaH_2 . Elemental analyses of $[Ni(fabt)_2]$ and $[Pd(fabt)_2]$ were performed at Osaka University and those of $[Zn(fabt)_2]$ and $[Hg(fabt)_2]$ at the Chemical Materials Center of the Institute for Molecular Science.

2-(Ferrocenyl)benzothiazoline was prepared according to the literature procedure.⁴

Syntheses.—Bis[2-(ferrocenylmethylenamino)benzenethio-

lato]nickel(II), $[Ni(fabt)_2]$. This deep red powder was prepared by heating 2-(ferrocenyl)benzothiazoline (0.81 g, 2.52 mmol) at $70^\circ C$ for 30 min with nickel(II) acetate tetrahydrate (0.31 g, 1.25 mmol) in ethanol (15 cm^3). Yield 79% based on nickel(II) acetate tetrahydrate. Slow recrystallisation from chloroform–ethanol in air is necessary to obtain X-ray-quality crystals. IR: 1589.5 cm^{-1} ($C=N$ stretch). NMR ($CDCl_3$): 1H (400 MHz), δ 7.68 (s, 2 H), 7.35 (d, 2 H), 6.98 (t, 2 H), 6.71 (t, 2 H), 6.52 (d, 2 H), 4.47 (m, 2 H), 4.42 (m, 2 H), 4.38 (m, 2 H), 4.35 (m, 2 H) and 4.22 (s, 10 H); ^{13}C (101 MHz), δ 165.28, 151.30, 145.58, 128.55, 127.55, 121.24, 116.81, 79.21, 72.59, 71.35, 70.56, 69.92 and 68.79 (Found: C, 57.85; H, 4.35; N, 4.00. Calc. for $C_{34}H_{28}Fe_2N_2S_2$: C, 58.40; H, 4.05; N, 4.00%).

Bis[2-(ferrocenylmethylenamino)benzenethiolato]zinc(II), $[Zn(fabt)_2]$. This red compound was prepared analogously to $[Ni(fabt)_2]$, by using zinc(II) acetate dihydrate. Yield 75% based on zinc(II) acetate dihydrate. X-Ray-quality crystals were best obtained in recrystallisations by slow evaporation of chloroform–methanol solutions in air. IR: 1589.5 cm^{-1} ($C=N$ stretch). NMR ($CDCl_3$): 1H (400 MHz), δ 8.13 (s, 2 H), 7.64 (d, 2 H), 7.10 (t, 2 H), 6.99 (t, 2 H), 6.94 (d, 2 H), 5.63 (m, 2 H), 4.45 (m, 2 H), 4.35 (m, 2 H), 4.28 (m, 2 H) and 4.22 (s, 10 H); ^{13}C (101 MHz), δ 165.59, 146.59, 142.25, 133.73, 127.44, 122.65, 118.15, 77.82, 73.98, 73.43, 69.65 and 68.95 (Found: C, 57.65; H, 4.25; N, 3.90. Calc. for $C_{34}H_{28}Fe_2N_2S_2Zn$: C, 57.85; H, 4.00; N, 3.95%).

Bis[2-(ferrocenylmethylenamino)benzenethiolato]palladium(II), $[Pd(fabt)_2]$. This deep red compound was prepared by the same procedure as for $[Ni(fabt)_2]$ by using palladium(II) acetate. Yield 76% based on palladium(II) acetate. X-Ray-quality crystals of the complex were obtained from chloroform–methanol solution in air. IR: 1601.1 cm^{-1} ($C=N$ stretch). NMR ($CDCl_3$): 1H (400 MHz), δ 7.75 (s, 2 H), 7.40 (d, 2 H), 7.01 (t, 2 H), 6.82 (t, 2 H), 6.81 (d, 2 H), 5.67 (m, 2 H), 4.44 (m, 2 H), 4.37 (m, 2 H), 4.24 (m, 2 H) and 4.17 (s, 10 H); ^{13}C (101 MHz), δ 162.68, 151.32, 146.18, 129.45, 127.84, 122.04, 117.58, 78.35, 73.49, 72.32, 71.48, 69.81 and 69.10 (Found: C, 54.25; H, 3.85; N, 3.75. Calc. for $C_{34}H_{28}Fe_2N_2PdS_2$: C, 54.70; H, 3.80; N, 3.75%).

Reactions.— $[Ni(fabt)_2]$ or $[Zn(fabt)_2]$ with $HgCl_2$. Mercury(II) chloride (0.09 g, 0.33 mmol) and $[Ni(fabt)_2]$ (0.23 g, 0.33 mmol) {or $[Zn(fabt)_2]$ (0.24 g, 0.34 mmol)} were dissolved in methanol (20 cm^3), and stirred at $70^\circ C$ for 30 min. Yield 52% {58% with $[Zn(fabt)_2]$ } based on $HgCl_2$. Recrystallisation from chloroform–ethanol solution in air gave orange crystals. IR: 1614.6 cm^{-1} ($C=N$ stretch). NMR ($CDCl_3$): 1H (400 MHz), δ 8.22 (s, 2 H), 7.60 (d, 2 H), 7.13 (t, 2 H), 7.09 (t, 2 H), 6.86

† Present address: Institute of Chemistry, College of General Education, Osaka University, Toyonaka, Osaka 560, Japan.

‡ Supplementary data available: see Instructions for Authors, *J. Chem. Soc., Dalton Trans.*, 1992, Issue 1, pp. xx–xxv.

Table 1 Crystallographic data

Complex	[Ni(fabt) ₂]	[Zn(fabt) ₂]	[Pd(fabt) ₂]	[Hg(fabt) ₂]
Formula	C ₃₄ H ₂₈ Fe ₂ N ₂ NiS ₂ ·2CHCl ₃	C ₃₄ H ₂₈ Fe ₂ N ₂ S ₂ Zn·CH ₃ OH	C ₃₄ H ₂₈ Fe ₂ N ₂ PdS ₂	C ₃₄ H ₂₈ Fe ₂ HgN ₂ S ₂
M	937.85	737.79	746.82	841.06
Crystal system	Monoclinic	Monoclinic	Orthorhombic	Triclinic
Space group	P2 ₁ /a	P2 ₁ /n	P2 ₁ 2 ₁ 2 ₁	P\bar{1}
a/Å	19.239(4)	16.569(4)	20.575(9)	9.566(2)
b/Å	20.072(5)	17.598(4)	12.349(3)	21.713(3)
c/Å	10.163(3)	10.575(1)	11.754(3)	7.320(2)
$\alpha/^\circ$				94.26(2)
$\beta/^\circ$		96.85(2)	94.80(2)	102.40(2)
$\gamma/^\circ$				92.48(2)
$U/\text{\AA}^3$	3896.6(97)	3072.7(42)	2986.3(17)	1478.0(34)
Z	4	4	4	2
$D_c/\text{g cm}^{-3}$	1.60	1.60	1.66	1.89
$\mu(\text{Mo-K}\alpha)/\text{cm}^{-1}$	17.6	18.9	17.1	63.1
$2\theta_{\max}/^\circ$	50	55	50	50
Crystal dimensions (mm)	0.25 × 0.25 × 0.40	0.20 × 0.35 × 0.55	0.25 × 0.25 × 0.45	0.15 × 0.25 × 0.55
No. of measured reflections	6029	5009	3006	4061
No. reflections used in refinement	3194 [$ F_o > 4\sigma(F_o)$]	3689 [$ F_o > 3\sigma(F_o)$]	2349 [$ F_o > 3\sigma(F_o)$]	2640 [$ F_o > 3\sigma(F_o)$]
No. of parameters	563	501	483	483
R	0.057	0.068	0.064	0.074
R'	0.062	0.075	0.053	0.086

* Weighting scheme 1/[$\sigma^2(F_o)$].

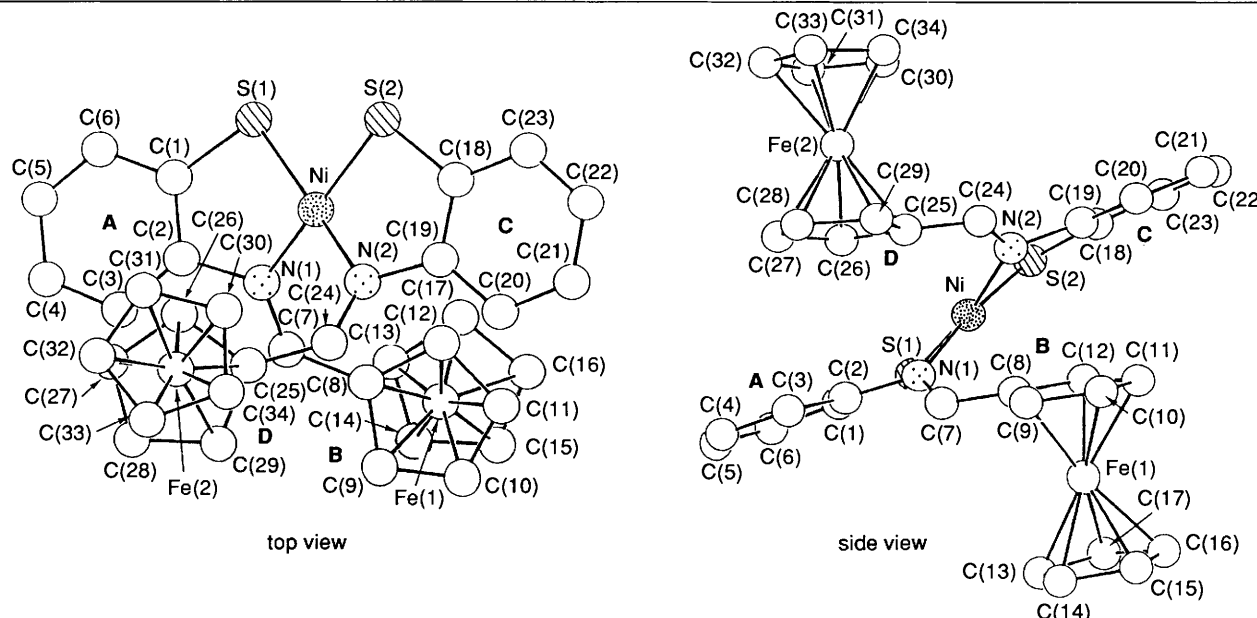


Fig. 1 Molecular structure of [Ni(fabt)₂]

(d, 2 H), 4.84 (m, 4 H), 4.36 (m, 4 H) and 4.19 (m, 10 H); ¹³C (101 MHz), δ 163.28, 150.49, 134.05, 132.74, 125.97, 125.39, 119.54, 78.93, 72.03, 70.11 and 69.46 (Found: C, 48.30; H, 3.30; N, 3.25. Calc. for C₃₄H₂₈Fe₂HgN₂S₂: C, 48.55; H, 3.35; N, 3.35%).

X-Ray Crystallography.—Data collection and processing. All crystals were attached to the end of a glass fibre and coated with epoxy. X-Ray measurements of [Ni(fabt)₂], [Zn(fabt)₂] and [Hg(fabt)₂] were made using a CAD4 diffractometer with Mo-K α radiation and of [Pd(fabt)₂] using a Rigaku AFC-5 diffractometer with Mo-K α radiation; ω -2θ scans were used. Crystallographic data are summarised in Table 1. Empirical absorption corrections were applied. The intensities of three standard reflections were monitored every 100 and showed no greater fluctuations during the data collection than expected from Poisson statistics.

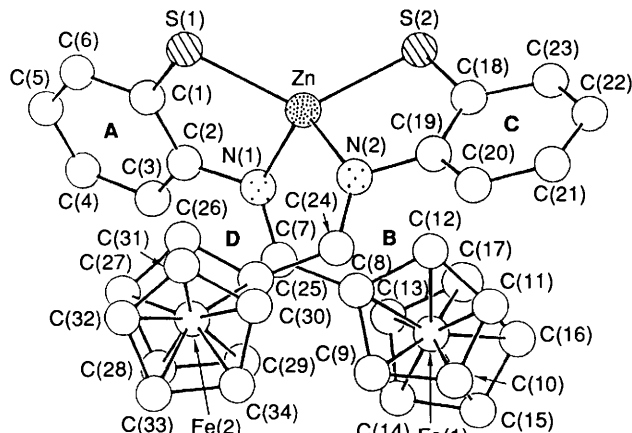
Structure analysis and refinement. The structure was solved by the use of MULTAN 80⁵ and refined by block-diagonal least squares with anisotropic thermal parameters for non-H atoms

and isotropic ones for H atoms. Atomic scattering factors and anomalous scattering coefficients were taken from ref. 6. All calculations were carried out using the program system UNICS III⁷ on a HITAC M680 Hitachi computer at the Computer Centre of the Institute for Molecular Science. Figs. 1–4 were drawn by the use of ORTEP.⁸ Final atom coordinates for the non-hydrogen atoms of [Ni(fabt)₂], [Zn(fabt)₂], [Pd(fabt)₂] and [Hg(fabt)₂] are given in Tables 2, 3, 4 and 5, respectively.

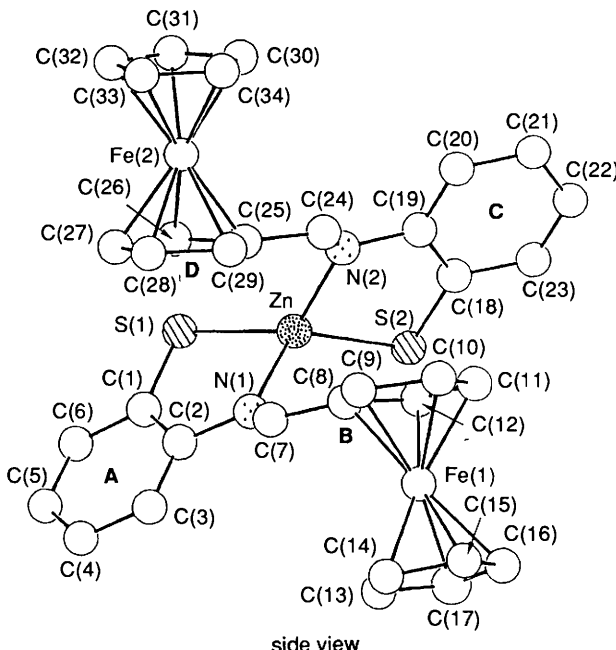
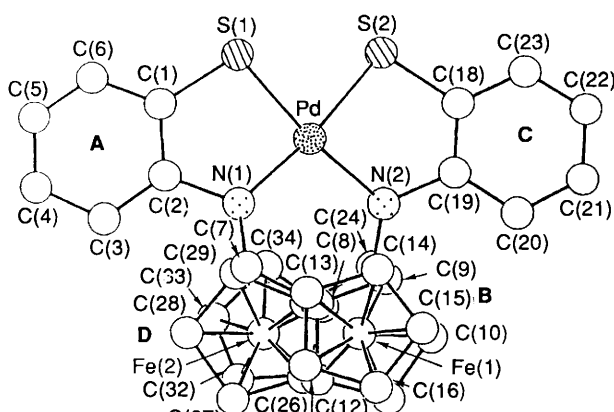
Additional material available from the Cambridge Crystallographic Data Centre comprises H-atom coordinates, thermal parameters and remaining bond lengths and angles.

Results and Discussion

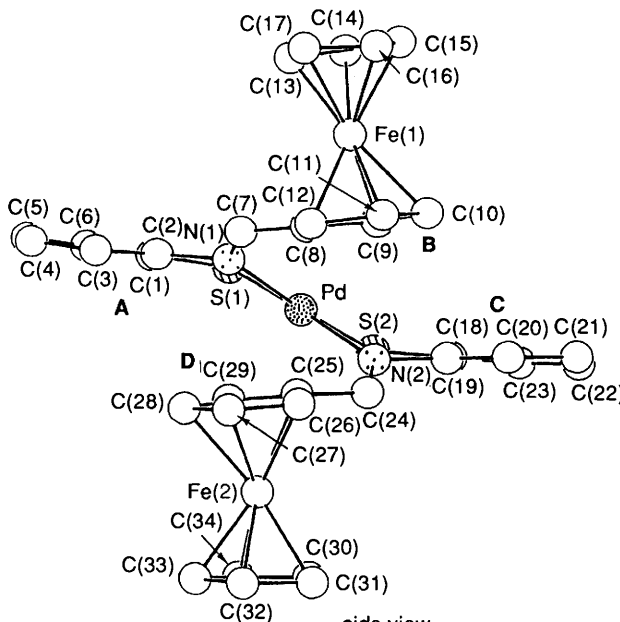
Syntheses.—The syntheses started from 2-(ferrocenyl)benzothiazoline, which was obtained from ferrocenecarbaldehyde and 2-aminothiophenol.⁴ The reaction of the appropriate [M(CH₃CO₂)₂] (M = Ni, Zn or Pd) with the benzothiazoline



top view

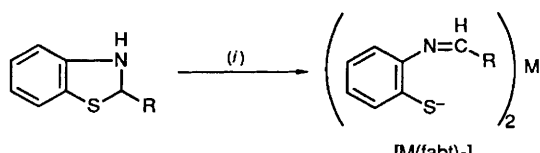
Fig. 2 Molecular structure of $[\text{Zn}(\text{fabt})_2]$ 

top view

Fig. 3 Molecular structure of $[\text{Pd}(\text{fabt})_2]$

(2 mol) gave the respective Schiff-base complex $[\text{M}(\text{fabt})_2]$ in generally very good yields (Scheme 1). Treatment of the $[\text{Ni}(\text{fabt})_2]$ or $[\text{Zn}(\text{fabt})_2]$ complex with HgCl_2 in methanol afforded $[\text{Hg}(\text{fabt})_2]$.

Molecular Structure of $[\text{Ni}(\text{fabt})_2]$.—The molecular structure

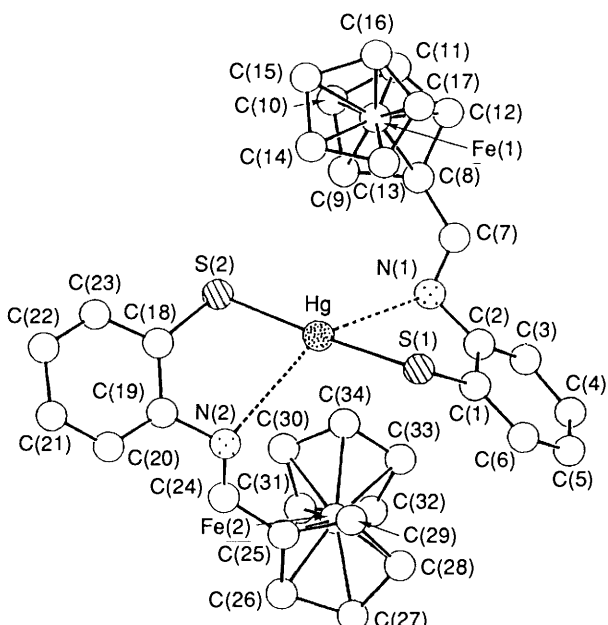


Scheme 1 R = Ferrocenyl; M = Ni, Zn or Pd. (i) $\text{M}(\text{CH}_3\text{COO}_2)_2$ in EtOH

and atomic numbering scheme of $[\text{Ni}(\text{fabt})_2]$ are shown in Fig. 1. Though strong interligand steric interactions occur, $[\text{Ni}(\text{fabt})_2]$ involves a slightly distorted square-planar *cis*-type co-ordination by 2S and 2N atoms of fabt ligands. The dihedral angle between the S-Ni-N planes is $10.8(2)^\circ$. Geometrical parameters are given in Table 6. The average Ni-S distance (2.165 \AA) falls in the range reported (2.14 – 2.21 \AA) for planar nickel(II) thiolate complexes.⁹ The average Ni-N distance (1.926 \AA) is relatively longer than reported Ni^{II} -N(imine) bond lengths of 1.83 – 1.92 \AA .¹⁰ Consequently the strain inherent in access of two bulky ferrocenyl groups is relieved by these elongated Ni^{II} -N bonds. The N-Ni-N bond angle, $98.4(3)^\circ$, is relatively wide and this result also supports the above argument (Table 6). Short intramolecular non-bonded contacts between two fabt ligands are found: C(7) ... C(24) 3.51(1), C(7) ... C(25) 3.35(1), C(8) ... C(24) 3.37(1) and C(8) ... C(25) 3.36(1) \AA

Table 2 Fractional atomic coordinates ($\times 10^4$) for $[\text{Ni}(\text{fabt})_2]$

Atom	X/a	Y/b	Z/c	Atom	X/a	Y/b	Z/c
Ni	1545(1)	2361(1)	419(1)	C(13)	3478(6)	4442(5)	425(11)
Fe(1)	3747(1)	3522(1)	-210(1)	C(14)	4012(6)	4508(6)	-409(13)
Fe(2)	775(1)	1447(1)	-3922(1)	C(15)	4584(6)	4144(6)	191(12)
Cl(1)	939(2)	4420(3)	4269(4)	C(16)	4430(6)	3850(6)	1339(12)
Cl(2)	1953(3)	4691(3)	2527(5)	C(17)	3722(6)	4027(6)	1517(11)
Cl(3)	2344(3)	4064(3)	4990(4)	C(18)	2158(5)	1119(5)	1529(9)
Cl(4)	3300(3)	2643(3)	4191(5)	C(19)	2403(4)	1222(4)	296(9)
Cl(5)	4332(2)	1854(3)	3241(5)	C(20)	2995(5)	872(4)	-25(9)
Cl(6)	3659(3)	1466(3)	5486(6)	C(21)	3298(5)	400(5)	841(10)
S(1)	862(1)	2992(1)	1433(3)	C(22)	3034(5)	284(5)	2042(10)
S(2)	1465(1)	1616(1)	1923(3)	C(23)	2455(5)	621(5)	2389(9)
N(1)	1659(3)	3113(3)	-708(6)	C(24)	1977(4)	1616(4)	-1792(8)
N(2)	2020(3)	1703(3)	-528(7)	C(25)	1522(4)	1961(4)	-2753(9)
C(1)	631(4)	3533(4)	112(9)	C(26)	831(4)	2221(4)	-2622(9)
C(2)	1038(4)	3532(4)	-957(8)	C(27)	530(5)	2443(5)	-3873(10)
C(3)	857(4)	3877(4)	-2124(9)	C(28)	1000(6)	2336(5)	-4804(9)
C(4)	256(5)	4277(5)	-2221(10)	C(29)	1620(5)	2023(5)	-4136(9)
C(5)	-132(5)	4311(5)	-1134(11)	C(30)	632(8)	533(5)	-3170(12)
C(6)	40(5)	3958(5)	-12(11)	C(31)	-14(7)	834(6)	-3560(12)
C(7)	2211(4)	3332(4)	-1238(9)	C(32)	-82(6)	971(6)	-4887(12)
C(8)	2897(5)	3019(5)	-1046(10)	C(33)	530(7)	759(6)	-5393(11)
C(9)	3392(5)	3140(6)	-2014(10)	C(34)	972(6)	491(5)	-4313(15)
C(10)	3995(5)	2802(6)	-1497(12)	C(35)	1712(6)	4151(7)	3691(11)
C(11)	3935(5)	2527(6)	-268(13)	C(36)	3545(8)	1868(8)	3948(13)
C(12)	3228(5)	2650(5)	67(10)				

**Fig. 4** Molecular structure of $[\text{Hg}(\text{fabt})_2]$

(Table 7). It is worth noting that, though each planar fabt ligand is in non-chiral, this complex shows a helical chirality.

Molecular Structure of $[\text{Zn}(\text{fabt})_2]$.—As is apparent from Fig. 2, the zinc atom has a distorted-tetrahedral geometry with a dihedral angle of $80.4(2)^\circ$ between the S–Zn–N planes (Table 8). The Zn–S and Zn–N bond distances are normal.^{11,12} The S(1)–Zn–S(2) bond angle [$123.4(1)^\circ$] is slightly larger than expected for tetrahedral geometry, while N(1)–Zn–N(2), $106.9(2)^\circ$, is close to the tetrahedral value. The bond angles S(1)–Zn–N(1) and S(2)–Zn–N(2), $88.7(2)$ and $89.7(2)^\circ$, with the constraints of an intraligand bite angle in the ‘2-aminothiophenol’, are smaller than the S–Zn–N angles found in other zinc complexes containing five-membered chelate ring systems (Table 6).¹² The most significant and noticeable feature is the twisting of the ligands into non-planar configurations to form

the helical arrangement. The interannular angles in the benzene rings and monosubstituted cyclopentadienyl rings are $55.2(3)^\circ$ (between rings A and B) and $58.8(3)^\circ$ (between rings C and D) and the corresponding angles of $[\text{Ni}(\text{fabt})_2]$ are $15.5(4)$ and $21.6(4)^\circ$ (Table 8). Furthermore, the distances between the ferrocenylmethyleneamino moieties of the ligands [C(7) ... C(24) $3.47(1)$, C(7) ... C(25) $3.21(1)$, C(8) ... C(24) $3.13(1)$ and C(8) ... C(25) $3.33(1)$ Å] are shorter than the corresponding distances of $[\text{Ni}(\text{fabt})_2]$ having a square-planar configuration (Table 7) and the dihedral angle, $14.5(4)^\circ$, between the two monosubstituted cyclopentadienyl rings in $[\text{Zn}(\text{fabt})_2]$ is smaller than that, $17.2(4)^\circ$, for $[\text{Ni}(\text{fabt})_2]$ (Table 8). It is apparent from these observations that the monohelical geometry results in a stacking interaction between the ferrocenylmethyleneamino moieties.

Molecular Structure of $[\text{Pd}(\text{fabt})_2]$.—A view of $[\text{Pd}(\text{fabt})_2]$ is shown in Fig. 3. The structure is similar to that of $[\text{Ni}(\text{fabt})_2]$ (Fig. 1).* The average Pd–S distance of 2.261 Å and the average Pd–N of 2.072 Å are normal (Table 6).¹³ The dihedral angle between the S–Pd–N planes is only $5.2(3)^\circ$. Furthermore, the benzene and cyclopentadienyl rings are approximately parallel with interplanar angles in the range $6.5(5)$ – $13.7(6)^\circ$ (Table 8). The molecular structure as a whole has substantial planar character. Short intramolecular non-bonded contacts between two fabt ligands are also found: C(7) ... C(24) $3.86(2)$, C(7) ... C(25) $3.43(2)$, C(8) ... C(24) $3.35(2)$ and C(8) ... C(25) $3.22(2)$ Å. The C(8) ... C(25) distance for this complex is 0.11 Å shorter, while the C(8) ... C(24) distance is 0.22 Å longer, than those for $[\text{Zn}(\text{fabt})_2]$ (Table 7). The space group, $P2_12_12_1$, and $Z = 4$ indicate that the crystals are spontaneously resolved.

Reactions of $[\text{M}(\text{fabt})_2]$ ($\text{M} = \text{Ni}, \text{Zn}$ or Pd) with HgCl_2 .—It is reported that the molecule HgCl_2 has a strong interaction with the cysteine thiolate group in living systems.¹⁴ We carried out the reaction of $[\text{M}(\text{fabt})_2]$ ($\text{M} = \text{Ni}, \text{Zn}$ or Pd) with HgCl_2 in 1:1 molar ratio to examine the co-ordination ability of the

* As suggested by one referee, $[\text{M}(\text{fabt})_2]$ ($\text{M} = \text{Ni}$ or Pd) can be considered also as planar species with bulky ligands pushing the planarity a little out of ideality.

Table 3 Fractional atomic coordinates ($\times 10^4$) for $[\text{Zn}(\text{fabt})_2]$

Atom	X/a	Y/b	Z/c	Atom	X/a	Y/b	Z/c
Zn	7 721(1)	8 223(1)	1 359(1)	C(15)	3 977(5)	6 959(5)	3 556(8)
Fe(1)	5 061(1)	7 175(1)	2 880(1)	C(16)	3 876(5)	7 482(5)	2 582(7)
Fe(2)	9 066(1)	5 712(1)	2 904(1)	C(17)	4 332(5)	8 115(5)	2 899(8)
S(1)	8 801(1)	8 879(1)	2 243(2)	C(18)	6 895(4)	7 753(4)	-1 121(6)
S(2)	6 932(1)	8 636(1)	-355(2)	C(19)	7 279(4)	7 097(4)	-629(6)
O(1)	6 240(13)	5 026(9)	5 326(14)	C(20)	7 291(5)	6 442(5)	-1 330(7)
N(1)	7 282(3)	8 158(3)	3 151(5)	C(21)	6 888(6)	6 389(5)	-2 540(7)
N(2)	7 681(3)	7 139(3)	619(5)	C(22)	6 447(6)	7 014(6)	-2 986(7)
C(1)	8 409(4)	9 009(4)	3 708(7)	C(23)	6 457(5)	7 678(5)	-2 328(7)
C(2)	7 715(4)	8 629(4)	4 063(6)	C(24)	7 697(4)	6 521(4)	1 277(6)
C(3)	7 413(5)	8 773(5)	5 229(7)	C(25)	8 139(4)	6 449(4)	2 544(6)
C(4)	7 831(5)	9 275(5)	6 085(7)	C(26)	8 827(5)	6 850(5)	3 048(7)
C(5)	8 524(5)	9 628(5)	5 770(7)	C(27)	9 051(6)	6 562(5)	4 253(8)
C(6)	8 803(5)	9 508(4)	4 602(8)	C(28)	8 510(6)	5 962(5)	4 499(7)
C(7)	6 847(4)	7 609(4)	3 553(6)	C(29)	7 931(5)	5 869(5)	3 436(7)
C(8)	6 288(4)	7 153(4)	2 762(6)	C(30)	9 295(5)	5 145(6)	1 284(7)
C(9)	5 990(4)	6 425(4)	3 147(7)	C(31)	9 991(5)	5 543(5)	1 757(7)
C(10)	5 426(5)	6 180(4)	2 149(8)	C(32)	10 211(4)	5 274(5)	2 970(7)
C(11)	5 357(5)	6 729(5)	1 187(7)	C(33)	9 661(5)	4 718(4)	3 297(7)
C(12)	5 874(4)	7 340(5)	1 552(6)	C(34)	9 094(5)	4 644(5)	2 226(8)
C(13)	4 732(5)	7 990(5)	4 099(8)	C(35)	5 288(14)	5 061(20)	5 351(30)
C(14)	4 509(5)	7 265(6)	4 523(7)				

Table 4 Fractional atomic coordinates ($\times 10^4$) for $[\text{Pd}(\text{fabt})_2]$

Atom	X/a	Y/b	Z/c	Atom	X/a	Y/b	Z/c
Pd	3 983(0)	7 185(1)	1 614(1)	C(15)	7 082(7)	6 740(15)	387(13)
Fe(1)	6 265(1)	7 507(1)	-110(2)	C(16)	7 163(6)	7 176(15)	-720(14)
Fe(2)	3 571(1)	10 992(2)	155(2)	C(17)	6 717(8)	6 726(13)	-1 453(13)
S(1)	3 489(2)	5 602(3)	1 192(3)	C(18)	4 182(6)	7 848(11)	4 069(12)
S(2)	3 647(2)	6 919(3)	3 427(4)	C(19)	4 489(6)	8 607(10)	3 446(12)
N(1)	4 262(4)	7 132(9)	-67(9)	C(20)	4 953(6)	9 279(11)	3 948(12)
N(2)	4 329(5)	8 656(9)	2 239(9)	C(21)	5 047(7)	9 227(13)	5 108(13)
C(1)	3 398(5)	5 882(10)	-248(12)	C(22)	4 706(8)	8 510(12)	5 749(12)
C(2)	3 772(7)	6 612(11)	-790(11)	C(23)	4 285(7)	7 819(12)	5 233(11)
C(3)	3 676(6)	6 890(12)	-1 931(11)	C(24)	4 391(6)	9 586(11)	1 703(13)
C(4)	3 196(8)	6 341(14)	-2 576(13)	C(25)	4 212(7)	9 815(11)	575(11)
C(5)	2 890(7)	5 492(14)	-2 061(13)	C(26)	4 530(7)	10 636(12)	-64(14)
C(6)	2 975(6)	5 263(11)	-952(14)	C(27)	4 237(9)	10 734(15)	-1 138(15)
C(7)	4 800(6)	7 481(11)	-616(11)	C(28)	3 694(9)	9 902(13)	-1 180(15)
C(8)	5 327(6)	8 074(11)	-6(12)	C(29)	3 705(6)	9 326(11)	-90(12)
C(9)	5 570(6)	7 964(12)	1 066(12)	C(30)	3 244(9)	11 701(17)	1 469(17)
C(10)	6 110(7)	8 646(12)	1 149(12)	C(31)	3 438(9)	12 487(12)	786(17)
C(11)	6 202(7)	9 147(12)	73(14)	C(32)	3 106(12)	12 336(19)	-186(18)
C(12)	5 737(7)	8 782(14)	-670(13)	C(33)	2 679(9)	11 651(20)	16(25)
C(13)	6 353(8)	6 007(12)	-808(15)	C(34)	2 746(9)	11 177(13)	1 102(20)
C(14)	6 581(7)	5 995(14)	290(17)				

sulfur atoms in $[\text{M}(\text{fabt})_2]$. The reactions of $[\text{Ni}(\text{fabt})_2]$ and $[\text{Zn}(\text{fabt})_2]$ in methanol with HgCl_2 result in a moderate yield of $[\text{Hg}(\text{fabt})_2]$ {52% with $[\text{Ni}(\text{fabt})_2]$ and 58% with $[\text{Zn}(\text{fabt})_2]$ } and attempts to cause $[\text{Pd}(\text{fabt})_2]$ to react produced $[\text{Hg}(\text{fabt})_2]$ in very small yield. The orange powder thus obtained was recrystallised from chloroform–ethanol and X-ray crystal structure determined (Fig. 4). The reaction product is a trinuclear mercury(II) complex, $[\text{Hg}(\text{fabt})_2]$, in which the mercury atom is in a linear *trans*- $[\text{Hg}^{\text{II}}\text{S}_2]$ type co-ordination having $\text{Hg}-\text{S}$ 2.345(4) and 2.329(4) Å and $\text{S}-\text{Hg}-\text{S}$ 174.0(1) $^\circ$. Moreover, secondary intramolecular interactions between the mercury and nitrogen atoms are found (Table 6).¹⁵ Thus the nickel and zinc atoms in the starting $[\text{Ni}(\text{fabt})_2]$ and $[\text{Zn}(\text{fabt})_2]$ complexes are clearly pushed out by the attack of the mercury atom. This result is correlated to the strong interaction of the mercury with the thiolate group in biochemistry. It is also noteworthy that a similar *trans*- $[\text{Hg}^{\text{II}}\text{S}_2\text{N}_2]$ structure around the mercury atom has been found in the mercury(II)-L-cysteine complex.¹⁶ As shown in Fig. 4, the fabt ligands of $[\text{Hg}(\text{fabt})_2]$ are markedly non-planar in contrast to

$[\text{M}(\text{fabt})_2]$ ($\text{M} = \text{Ni}, \text{Zn}$ or Pd) complexes showing helical chirality.

Spectroscopic Characterization of the Compounds.—The IR spectra show the typical bands of co-ordinated imines. The wavenumbers corresponding to $\nu(\text{C}=\text{N})$ are included in Experimental section. It should be noted that these values cannot be correlated to the $\text{C}=\text{N}$ bond lengths: the imine $\text{C}=\text{N}$ bond distances [1.32(2) and 1.35(2) Å] of $[\text{Pd}(\text{fabt})_2]$ are marginally longer than the corresponding bonds in $[\text{Ni}(\text{fabt})_2]$ [1.29(1) and 1.32(1) Å] and $[\text{Zn}(\text{fabt})_2]$ [1.29(1) and 1.30(1) Å] (Table 6), but the imine stretch (1601.1 cm⁻¹) of $[\text{Pd}(\text{fabt})_2]$ is higher than those corresponding to $[\text{Ni}(\text{fabt})_2]$ and $[\text{Zn}(\text{fabt})_2]$ (both 1589.5 cm⁻¹). This suggests some difference in non-bonded interaction between two fabt ligands, as confirmed by the X-ray analyses (Table 7).

Proton NMR spectra of the compounds in CDCl_3 solution are reported in Experimental section. First it is to be noted that the appearance of only one azomethine signal for each compound as well as the presence of four benzene aromatic

Table 5 Fractional atomic coordinates ($\times 10^4$) for $[\text{Hg}(\text{fabt})_2]$

Atom	X/a	Y/b	Z/c	Atom	X/a	Y/b	Z/c
Hg	5 251(1)	2 793(0)	1 915(1)	C(15)	2 848(21)	4 722(7)	4 408(23)
Fe(1)	3 046(2)	3 936(1)	5 852(3)	C(16)	1 486(18)	4 494(8)	4 793(20)
Fe(2)	8 467(3)	1 198(1)	3 179(4)	C(17)	1 133(17)	3 904(9)	4 037(21)
S(1)	3 342(4)	2 065(2)	641(6)	C(18)	7 698(15)	3 666(6)	1 096(24)
S(2)	6 983(4)	3 594(2)	3 077(6)	C(19)	8 114(14)	3 169(6)	-1(19)
N(1)	4 329(13)	2 320(5)	4 955(16)	C(20)	8 789(16)	3 291(7)	-1 472(22)
N(2)	7 691(13)	2 559(5)	352(17)	C(21)	9 059(18)	3 874(8)	-1 917(25)
C(1)	3 596(16)	1 517(6)	2 421(19)	C(22)	8 729(15)	4 380(7)	-815(24)
C(2)	3 928(17)	1 694(7)	4 358(31)	C(23)	8 103(15)	4 267(7)	619(21)
C(3)	4 026(18)	1 249(7)	5 572(25)	C(24)	8 542(16)	2 150(7)	349(22)
C(4)	3 717(19)	631(7)	4 914(25)	C(25)	8 199(18)	1 518(6)	580(22)
C(5)	3 318(20)	456(7)	3 025(33)	C(26)	9 246(21)	1 056(8)	787(30)
C(6)	3 242(18)	884(7)	1 818(26)	C(27)	8 578(19)	475(7)	1 202(23)
C(7)	3 632(15)	2 559(6)	6 071(21)	C(28)	7 053(18)	597(7)	1 281(22)
C(8)	3 847(16)	3 165(6)	7 030(21)	C(29)	6 942(16)	1 245(6)	829(22)
C(9)	5 018(16)	3 623(7)	7 000(24)	C(30)	9 359(26)	1 901(8)	5 170(31)
C(10)	4 748(19)	4 171(7)	8 126(22)	C(31)	10 132(19)	1 333(11)	5 423(28)
C(11)	3 450(22)	4 050(7)	8 673(22)	C(32)	9 132(25)	896(9)	5 780(32)
C(12)	2 913(17)	3 442(7)	8 066(20)	C(33)	7 775(23)	1 153(8)	5 666(28)
C(13)	2 115(18)	3 711(7)	3 140(26)	C(34)	7 987(23)	1 759(9)	5 290(30)
C(14)	3 251(20)	4 215(9)	3 360(22)				

Table 6 Selected bond distances (\AA) and angles ($^\circ$) in $[\text{M}(\text{fabt})_2]$ ($\text{M} = \text{Ni}, \text{Zn}, \text{Pd}$ or Hg)

	$[\text{Ni}(\text{fabt})_2]$	$[\text{Zn}(\text{fabt})_2]$	$[\text{Pd}(\text{fabt})_2]$	$[\text{Hg}(\text{fabt})_2]$
M–S(1)	2.172(3)	2.266(2)	2.258(4)	2.345(4)
M–S(2)	2.157(3)	2.264(2)	2.264(4)	2.329(4)
M–N(1)	1.924(7)	2.089(5)	2.059(10)	2.808(13)*
M–N(2)	1.928(7)	2.062(5)	2.085(11)	2.860(14)*
N(1)–C(7)	1.323(11)	1.298(9)	1.352(16)	1.259(20)
N(2)–C(24)	1.290(11)	1.290(9)	1.316(18)	1.231(19)
S(1)–M–S(2)	88.3(1)	123.4(1)	86.8(2)	174.0(1)
S(1)–M–N(1)	86.7(2)	88.7(2)	83.5(3)	73.2(2)
S(1)–M–N(2)	170.5(2)	128.9(2)	170.2(3)	111.2(2)
S(2)–M–N(1)	171.5(2)	121.5(2)	169.7(3)	108.5(2)
S(2)–M–N(2)	87.5(2)	89.7(2)	84.2(3)	72.2(2)
N(1)–M–N(2)	98.4(3)	106.9(2)	105.7(4)	131.6(3)

* Intramolecular interaction.

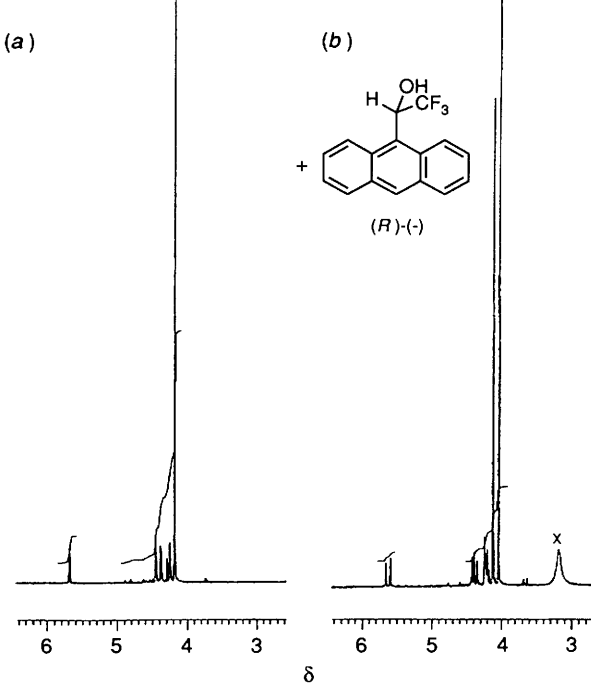
Table 7 Interatomic contacts (\AA)

	$[\text{Ni}(\text{fabt})_2]$	$[\text{Zn}(\text{fabt})_2]$	$[\text{Pd}(\text{fabt})_2]$
C(7) ... C(24)	3.51(1)	3.47(1)	3.86(2)
C(7) ... C(25)	3.35(1)	3.21(1)	3.43(2)
C(8) ... C(24)	3.37(1)	3.13(1)	3.35(2)
C(8) ... C(25)	3.36(1)	3.33(1)	3.22(2)

Table 8 Least-squares plane calculations

Angles between planes ($^\circ$)	$[\text{Ni}(\text{fabt})_2]$	$[\text{Zn}(\text{fabt})_2]$	$[\text{Pd}(\text{fabt})_2]$
S(1)–M–N(1)–S(2)–M–N(2)	10.8(2)	80.4(2)	5.2(3)
Stacking angles ($^\circ$)			
A–B	15.5(4)	55.2(3)	9.5(6)
C–D	21.6(4)	58.8(3)	13.7(6)
A–C	5.9(3)	86.5(3)	6.5(5)
B–D	17.2(4)	14.5(4)	8.0(7)

protons support the C_2 symmetrical structure. The ^1H NMR spectra of $[\text{Ni}(\text{fabt})_2]$, $[\text{Zn}(\text{fabt})_2]$ and $[\text{Pd}(\text{fabt})_2]$ showed five resonances in the cyclopentadienyl region. The high-field sharp peaks (δ 4.17–4.22) result from the non-substituted cyclopentadienyl rings. Since monosubstituted cyclopentadienyl ligands normally provide just two proton resonances, the

**Fig. 5** The ^1H NMR spectra for cyclopentadienyl rings of (a) $[\text{Pd}(\text{fabt})_2]$ and (b) $[\text{Pd}(\text{fabt})_2]$ in the presence of Pirkle's reagent

observation of the residual four signals suggests the existence of a certain rotational barrier involving the ferrocenyl groups. Moreover, small but significant downfield shifts are clearly observed for $[\text{Zn}(\text{fabt})_2]$ (δ 5.63) and $[\text{Pd}(\text{fabt})_2]$ (δ 5.67) compared with the corresponding signal of the same fragment in $[\text{Ni}(\text{fabt})_2]$ (δ 4.47). This deshielding indicates that the ferrocenyl–ferrocenyl distance of $[\text{Zn}(\text{fabt})_2]$ and $[\text{Pd}(\text{fabt})_2]$ in solution is also shorter than that of $[\text{Ni}(\text{fabt})_2]$, as independently shown by the X-ray analyses (Table 7). On the other hand, the protons of the monosubstituted cyclopentadienyl in $[\text{Hg}(\text{fabt})_2]$ appear as two singlets. This indicates that the rotation of ferrocenyl groups is not hindered about the C(7)–C(8) or C(24)–C(25) bond. Addition of one enantiomer of Pirkle's reagent¹⁷ [9 -(1-hydroxy-2,2,2-trifluoroethyl)anthracene] to a solution of $[\text{Ni}(\text{fabt})_2]$, $[\text{Zn}(\text{fabt})_2]$ or $[\text{Pd}(\text{fabt})_2]$ in CDCl_3 leads to splitting of some proton NMR

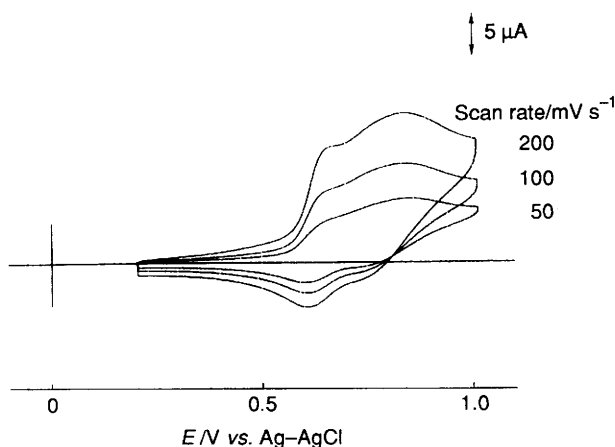


Fig. 6 Cyclic voltammogram of $[\text{Pd}(\text{fabt})_2]$ in acetonitrile solution (0.5 mmol dm^{-3})

signals, demonstrating the presence of two diastereomeric species; consequently, these complexes must have a chiral structure in solution (Fig. 5). For $[\text{Hg}(\text{fabt})_2]$ no splitting of peaks was observed even after addition of a large amount of Pirkle's reagent, in agreement with the achiral structure of $[\text{Hg}(\text{fabt})_2]$. The absorption spectra of $[\text{M}(\text{fabt})_2]$ ($\text{M} = \text{Ni}, \text{Pd}, \text{Zn}$ or Hg) in CHCl_3 are adequately summarized by the following $v_{\max}/10^3 \text{ cm}^{-1}$ ($\log \epsilon/\text{dm}^3 \text{ mol}^{-1} \text{ cm}^{-1}$) data: 19.70 (3.65) and 26.00 (3.61) for $[\text{Ni}(\text{fabt})_2]$, 20.30 (3.83) and 26.90 (3.93) for $[\text{Pd}(\text{fabt})_2]$, 20.40 (3.75) and 25.00 (3.82) for $[\text{Zn}(\text{fabt})_2]$ and 21.10 (3.58) and 27.70 (4.06) for $[\text{Hg}(\text{fabt})_2]$. The absorption spectra of these complexes are quite similar to each other over the whole region except for that of $[\text{Hg}(\text{fabt})_2]$. Thus the spectra of the complexes showing helical chirality is characterised by the two intense absorption bands at *ca.* 20 000 and *ca.* 26 000 cm^{-1} .

Cyclic Voltammetry.—The complexes $[\text{M}(\text{fabt})_2]$ ($\text{M} = \text{Ni}, \text{Pd}, \text{Zn}$ or Hg) contain two ferrocene units as redox-active centres and the redox properties have been investigated by cyclic voltammetry. Each of $[\text{Zn}(\text{fabt})_2]$ and $[\text{Hg}(\text{fabt})_2]$ shows a reversible oxidation process attributable to a ferrocene–ferrocenium couple, at 0.79 and 0.72 V respectively. The cyclic voltammogram for $[\text{Ni}(\text{fabt})_2]$ shows two oxidation potentials at 0.61 and 0.67 V at a scan rate of 50 mV s^{-1} , though at higher scan rates it shows only one oxidation potential at 0.68 V. Under the same conditions, bis[2-(phenylmethylenamino)-benzenethiolato]nickel(II), $[\text{Ni}(\text{pabt})_2]$, in which the ferrocenyl groups of $[\text{Ni}(\text{fabt})_2]$ are replaced by phenyl groups, is oxidised at 0.76 V.¹⁸ Thus one of two oxidation potentials for $[\text{Ni}(\text{fabt})_2]$ is attributable to the $\text{Ni}^{III}–\text{Ni}^{II}$ couple. The complex $[\text{Pd}(\text{fabt})_2]$ shows two oxidation potentials at 0.65 and 0.84 V at scan rates from 50 to 200 mV s^{-1} (Fig. 6). However, no peaks corresponding to the oxidation process of the $\text{Pd}^{III}–\text{Pd}^{II}$ couple ($E \leq 1.40 \text{ V}$) are observed for $[\text{Pd}(\text{pabt})_2]$.¹⁹ Therefore, the two oxidation processes in $[\text{Pd}(\text{fabt})_2]$ correspond to $\text{Fe}^{III}–\text{Fe}^{II}$ couples and this observation indicates that there is significant interaction between the two ferrocene units. The peculiarity of $[\text{Pd}(\text{fabt})_2]$ may be also correlated to some difference in non-bonded interaction between the two fabt ligands based on the difference in the interatomic contact site (Fig. 3 and Table 7).

Acknowledgements

The authors thank Dr. H. Nagao for valuable suggestions. This work was partially supported by Grant-in-Aid for Scientific Research No. 03640534 (to Y. K.) from the Ministry of Education, Science and Culture.

References

- P. L. Anelli, P. R. Ashton, R. Ballardini, V. Balzani, M. Delgado, M. T. Gandolfi, T. T. Goodnow, A. E. Kaiser, D. Philp, M. Pietraszkiewicz, L. Prodi, M. V. Reddington, A. M. Z. Slawin, N. Spencer, J. F. Stoddart, C. Vicent and D. J. Williams, *J. Am. Chem. Soc.*, 1992, **114**, 193; A. F. Williams, C. Piguet and G. Bernardinelli, *Angew. Chem., Int. Ed. Engl.*, 1991, **30**, 1490; E. C. Constable, *Angew. Chem., Int. Ed. Engl.*, 1991, **30**, 1450; P. R. Ashton, C. L. Brown, E. J. T. Chrystal, K. P. Parry, M. Pietraszkiewicz, N. Spencer and J. F. Stoddart, *Angew. Chem., Int. Ed. Engl.*, 1991, **30**, 1042; O. J. Gelling, F. van Bolhuis and B. L. Feringa, *J. Chem. Soc., Chem. Commun.*, 1991, 917; E. C. Constable, M. D. Ward and D. A. Tocher, *J. Chem. Soc., Dalton Trans.*, 1991, 1675; M.-T. Youinou, R. Ziessel and J.-M. Lehr, *Inorg. Chem.*, 1991, **30**, 2144; E. C. Constable, S. M. Elder, P. R. Raithby and M. D. Ward, *Polyhedron*, 1991, **10**, 1395.
- C. Deuschel-Cornioley, H. Stoeckli-Evans and A. von Zelewsky, *J. Chem. Soc., Chem. Commun.*, 1990, 121; L. F. Lindoy and D. H. Busch, *J. Chem. Soc., Chem. Commun.*, 1972, 683.
- T. Kawamoto and Y. Kushi, *Chem. Lett.*, 1992, 297.
- P. J. Palmer, R. B. Trigg and J. V. Warrington, *J. Med. Chem.*, 1971, **14**, 248.
- P. Main, S. J. Fiske, S. E. Hull, L. Lessinger, G. Germain, J.-P. Declercq and M. M. Woolfson, MULTAN 80, A System of Computer Programs for the Automatic Solution of Crystal Structures from X-Ray Diffraction Data, Universities of York and Louvain, 1980.
- International Tables for X-Ray Crystallography*, Kynoch Press, Birmingham, 1974, vol. 4.
- T. Sakurai and K. Kobayashi, *Sci. Rep. Inst. Chem. Phys. Res. Jpn.*, 1979, **55**, 69.
- C. K. Johnson, ORTEP, Report ORNL-3794, Oak Ridge National Laboratory, Oak Ridge, TN, 1965.
- N. Baidya, M. M. Olmstead and P. K. Mascharak, *Inorg. Chem.*, 1991, **30**, 3967 and refs. therein; H.-J. Krüger, G. Peng and R. H. Holm, *Inorg. Chem.*, 1991, **30**, 734.
- E. M. Martin, R. D. Bereman and P. Singh, *Inorg. Chem.*, 1991, **30**, 957 and refs. therein.
- D. T. Corwin, jun. and S. A. Koch, *Inorg. Chem.*, 1988, **27**, 493.
- W. J. Hu, D. Barton and S. J. Lippard, *J. Am. Chem. Soc.*, 1973, **95**, 1170 and refs. therein.
- T. Glowik and T. Ciszewska, *Acta Crystallogr., Sect. B*, 1982, **38**, 1735; A. S. Hirschon, W. K. Musker, M. M. Olmstead and J. L. Dallas, *Inorg. Chem.*, 1981, **20**, 1702; H. I. Heitner and S. J. Lippard, *Inorg. Chem.*, 1974, **13**, 815.
- K. Nordling, *Prog. Med. Chem.*, 1990, **27**, 189.
- E. Block, M. Brito, M. Gernon, D. McGowty, H. Kang and J. Zubietta, *Inorg. Chem.*, 1990, **29**, 3172; J. Bravo, J. S. Casas, M. V. Castano, M. Gayoso, Y. P. Mascarenhas, A. Sanchez, C. O. P. Santos and J. Sordo, *Inorg. Chem.*, 1985, **24**, 3435; A. Castineiras, W. Hiller, J. Strahle, J. Bravo, J. S. Casas, M. Gayoso and J. Sordo, *J. Chem. Soc., Dalton Trans.*, 1986, 1945.
- N. J. Taylor and A. J. Carty, *J. Am. Chem. Soc.*, 1977, **99**, 6143.
- W. H. Pirkle and M. S. Hoekstra, *J. Am. Chem. Soc.*, 1976, **98**, 1832.
- T. Kawamoto and Y. Kushi, *Chem. Lett.*, 1992, 893.
- T. Kawamoto and Y. Kushi, unpublished work.

Received 20th March 1992; Paper 2/01478E